Acta Cryst A FOUNDATIONS ADVANCES

ISSN 2053-2733

Testing of a 'hard' X-ray interferometer for experimental investigations

Tigran H. Eyramjyan,[a]* Mesrop H. Mesropyan,[b] Tamara S. Mnatsakanyan[a] and Minas K. Balyan[a]

[a]Faculty of Physics, Yerevan State University, Alex Manoogian 1, Yerevan 0025, Armenia, and [b]Faculty of Agrarian Engineering, Armenian National Agrarian University, Teryan 74, Yerevan 0009, Armenia. *Correspondence e-mail: tigeyro@ysu.am

Received 25 October 2019
Accepted 19 February 2020

Edited by I. A. Vartaniants, Deutsches Electronen-Synchrotron, Germany

Keywords: X-rays; LLL interferometer; 'hard' LLL interferometer; moiré fringes.

A 'hard' X-ray LLL interferometer is tested for experimental investigations. The interferometer has both a base and a 'ceiling', which are rigidly connected through columns. As a result, the interferometer does not have uncontrollable preliminary moiré. The intensity distribution is uniform in the interfering beams. It is shown that the interferometer is very sensitive to minor mechanical stresses. As a result, the interferometer must be freely placed on the goniometer head. Constant-thickness fringes are obtained using a wedge with a vertically placed apex. The volumes available for specimen placement are limited due to the existence of the ceiling. These difficulties can be overcome. The hard interferometer can be used for object and deformation investigations.

1. Introduction

X-rays in the region of 1 Å in wavelength can penetrate into a specimen, and thus the phase and amplitude information obtained from the specimen can be used to investigate the specimen's properties, making such investigations more effective. Another important property of X-rays with such wavelength is Bragg diffraction in crystals. Bragg diffraction has become the basis for various investigation methods: X-ray topography (Authier, 2001; Pinsker, 1982), the phase-contrast method (Ingal & Beliaevskaya, 1995) and more.

The interferometric method is one of the commonly used methods of material and deformation investigations based on dynamical diffraction of X-rays. The X-ray LLL (Laue–Laue–Laue) interferometer is widely used, as proposed by Bonse & Hart (1965*a*,*b*). It consists of three crystalline plates on a common base (Fig. 1). The plates are sufficiently thick ($\mu T >> 1$) so that only a weakly absorbing mode of the dispersion surface may pass through the plates (μ is the absorption coefficient of X-rays in the plates and T is the thickness of the interferometer plates). The incident beam falling on the first plate of the interferometer at the exact Bragg angle splits into two beams: transmitted and diffracted. This plate is called the splitter (S). The two beams thus formed, falling on the second mirror plate (M), give rise to two beams originating from sections M_1 and M_2. These beams interfere in the third analyser plate (A). Beams C and D emerging from plate A give rise to interference fringes called moiré fringes. If the phase difference between the interfering beams is zero, there are no moiré fringes in beams C and D. Moiré fringes can be introduced by forming a spatial phase gradient between the interfering beams, and this can be done by placing a specimen in the path of the interfering beams or by introducing deformations in the plates.

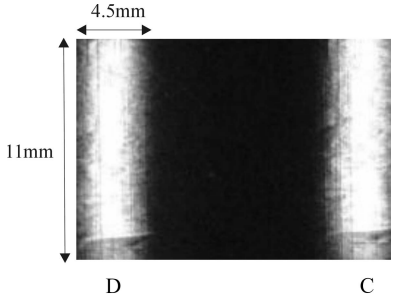

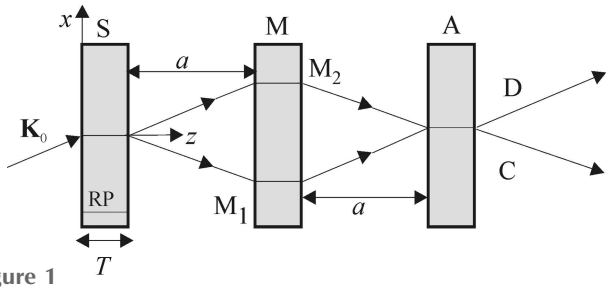

Figure 1
Diagram of an X-ray three-plate interferometer. $\mathbf{K}_0$ is the wavevector of the incident wave, RP the reflecting lattice planes, T the thickness of the plates, x and z the coordinates, S the splitter, M the mirror (with M_1 and M_2 regions), A the analyser plate, a the distance between the plates, and C and D the beams emerging from the interferometer.

Determination of the refractive index is performed by placing a wedge-shaped specimen in the path of one of the interfering beams. The refractive index is determined by measuring the spacing between the moiré fringes. If one introduces deformations in one of the plates of the interferometer (for example, if one introduces a dislocation, or irradiates the mirror block with electrons, γ-radiation or laser radiation), moiré fringes will be formed, and by measuring the local periods the deformations may be determined. Another important application of the LLL interferometer is the investigation of a specimen by the Momose X-ray phase-contrast computer tomography method (Momose, 1995). We would like to mention here the work of Eyramjyan *et al.* (2018), in which an LLL interferometer with a wedge-shaped mirror plate was proposed. In that work, the corresponding theory of moiré fringe formation is also presented. In all cases, the LLL interferometer has a preliminary moiré, which is caused by the deformations arising in the fabrication process. Such a type of moiré is not controllable and gives rise to difficulties for the investigation of deformations or object properties.

The X-ray interferometer, consisting of three crystalline plates, is very sensitive not only to deformations introduced into these plates, but also to deformations formed in the plates during the fabrication process. Up to now, all X-ray interferometers have had a preliminary moiré connected with the deformations formed during the fabrication process. Usually, the effect of the preliminary moiré is taken into account by means of the fringe scanning method (Momose & Hirano, 1999). In this method, the object and deformation phases are summed in the intensity distribution, and therefore the intensity distributions obtained with and without an object allow the application of the fringe scanning method. Meanwhile, Balyan (2016*a*,*b*) proposed coherent interferometric Fresnel and Fourier holography schemes, in which the phases of the deformation and the object cannot simply be summed in the expression of the intensity. Therefore the method of fringe scanning cannot be used in coherent holographic schemes.

Alternatively, the problem of preliminary moiré can be overcome by having an interferometer without preliminary moiré, which can be used to investigate deformations or objects. Rostomyan *et al.* (1989) suggested a 'hard' LLL X-ray interferometer that has no preliminary moiré. This interferometer, besides the common base, has also a 'ceiling,' which fixes all three plates [Fig. 2(*a*)] and for this reason we call such an interferometer a 'hard' interferometer. This provides zero influence of the deformations arising during the fabrication process. As a result the interferometer has no preliminary moiré. The names 'base' and 'ceiling' are used relatively. That is, the interferometer can be placed on the goniometer head with the base or the ceiling at the bottom. Photographs of the usual LLL and the 'hard' X-ray interferometer are shown in Figs. 3(*a*) and 3(*b*), respectively.

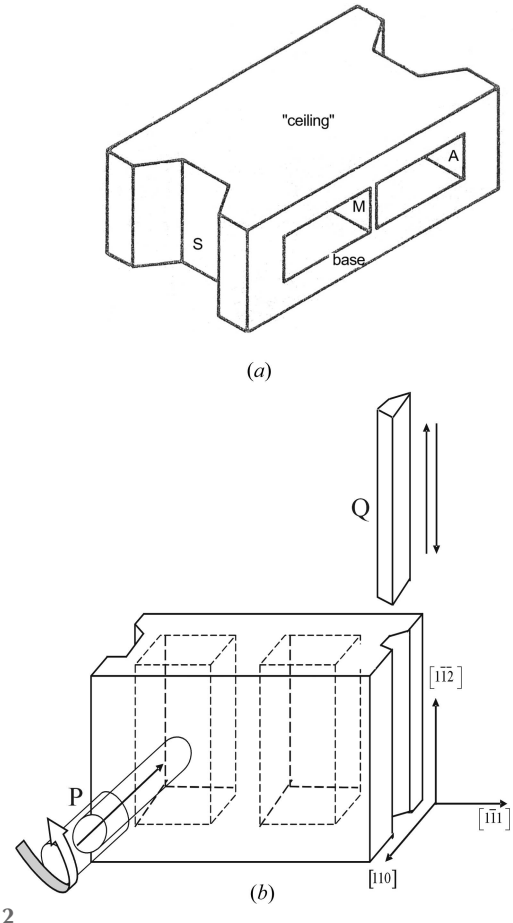

Figure 2
The scheme and fabrication process of the new three-plate hard X-ray LLL interferometer. The ray trajectories are the same as in the standard interferometer in Fig. 1. (*a*) A schematic view of the hard interferometer. S is the splitter plate, M the mirror plate and A the analyser plate of the hard interferometer. The hard interferometer, unlike the standard one in Fig. 1, has a base and a ceiling, which fixes its plates together. (*b*). The fabrication process. P is the rotating copper tube and Q a metallic plate of a special form.

The aim of our work is to test this hard X-ray interferometer for conducting experimental studies without preliminary moiré. Moreover, the hard X-ray interferometer will be compared with the conventional one in terms of physical research. Our goal is to use this type of interferometer in the future to study objects and deformations. We think it will be interesting for researchers to compare the results obtained with such an interferometer with the results obtained

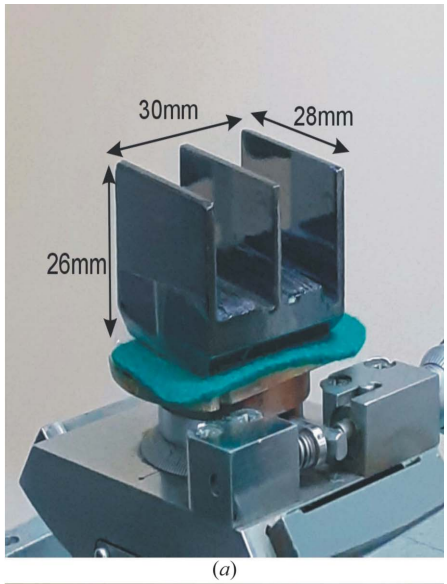

(*a*)

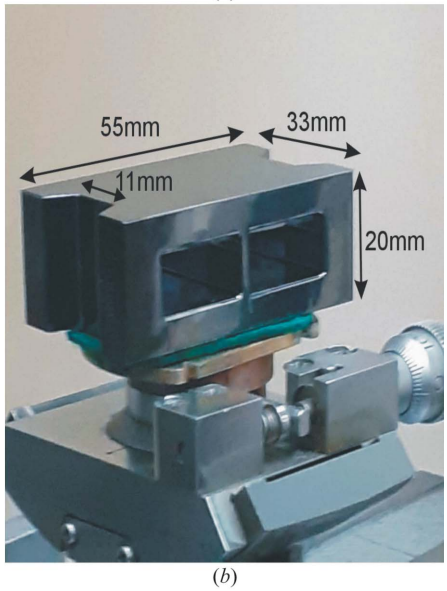

(*b*)

Figure 3
Photographs of X-ray interferometers. (*a*) The usual LLL form and (*b*) the new hard LLL interferometer.

by a conventional interferometer using the fringe scanning method.

2. Experiment

Our experiments are performed using a hard X-ray interferometer [Figs. 2 and 3(*b*)]. The interferometer is fabricated for Mo $K\alpha_1$ radiation and for Si(220) symmetrical Laue-case reflection using a dislocation-free monolithic float zone (FZ) silicon crystal. As a preliminary step, a cubic form crystal was cut, strongly keeping the crystallographic directions, to high accuracy. Then the interferometer blocks were manually fabricated. In contrast to the usual LLL interferometer, the hard interferometer has two cavities. In Fig. 2(*b*) the fabrication process of these cavities is shown. A high-frequency rotating copper cylindrical tube P is used. Simultaneously with

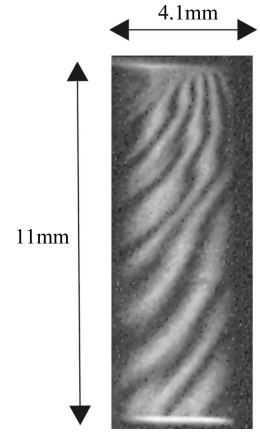

Figure 4
The uncontrolled preliminary moiré pattern in beam C (see Fig. 1) from a standard X-ray LLL interferometer. The interferometer has been scanned along the direction *Ox*.

the tube, abrasive powder is used. After drilling the two cylindrical holes, these cylindrical holes are reduced to a rectangular form by means of metallic plates and an abrasive powder. Concurrently, the perfect geometry of the interferometer is kept. A metallic plate Q of a special form is used with abrasive powder for the fabrication of the dimples on the S and A plates. The dimensions of the interferometer plates, their thicknesses and the inter-plate distances are fabricated with an accuracy of 3–4 µm. The dimensions and above-mentioned parameters are measured using a comparator, which allows measurements to be taken with the mentioned accuracy.

Chemical processing is performed by standard methods, using a multicomponent etchant for the Si crystal. The thicknesses T of the plates are approximately 2 mm. For each plate we have $\mu T \simeq 3$, where $\mu = 1.42\ \text{mm}^{-1}$ is the linear absorption coefficient.

An X-ray laboratory source was used. The size of the source is 0.4 mm in the diffraction plane. The length of the collimator of the X-ray chamber is 0.4 m, and the width of the beam incident on the interferometer in the diffraction plane is 0.3 mm. The experiments were performed at 40 kV and 20 mA.

First, we obtained the moiré pattern, using a standard LLL X-ray interferometer (Fig. 4). This interferometer shows a

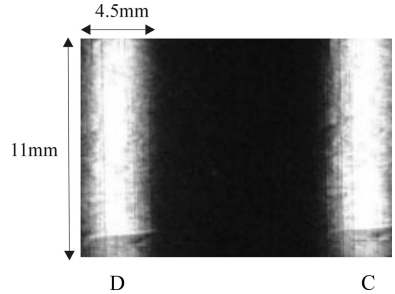

Figure 5
The uniform intensity distribution obtained in beams C and D (see Fig. 1) using the hard X-ray LLL interferometer. The interferometer has been scanned along the direction *Ox*.

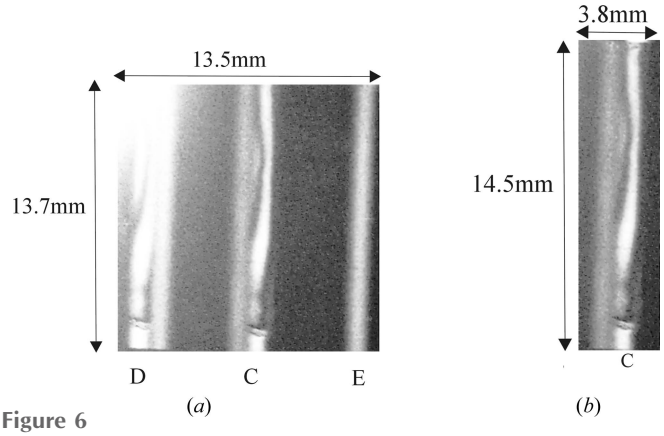

Figure 6
Moiré fringes appearing in the hard X-ray interferometer due to the attachment of the interferometer to the goniometer head with a thin adhesive layer. (*a*) The intensity distribution in the interfering beams C and D and in a non-interfering beam E. (*b*). The intensity distribution in beam C.

preliminary uncontrollable moiré in beam C (see Fig. 1). In comparison with this interferometer, the hard X-ray interferometer does not have any preliminary uncontrollable moiré (Fig. 5). Note that for Figs. 4 and 5 the interferometers were scanned along the direction *Ox* simultaneously with the photographic film. The incident beam is fixed. As a result, the regions of the interference patterns are increased by more than 4 mm. The intensity distribution obtained by the hard X-ray interferometer is almost uniform. It should be noted that the hard interferometer was placed on the goniometer head without mounting (freely) or using only a weakly sticking substance. This is essential because the hard interferometer is very sensitive to even minor mechanical stresses that may occur during fastening. As an example, Fig. 6 shows the moiré which was obtained with the hard interferometer attached to the goniometer head with a thin layer of adhesive. In Fig. 6(*a*) the intensity distributions in the interfering beams C and D and in a non-interfering beam E are shown. In Fig. 6(*b*) the intensity distribution in beam C is shown separately.

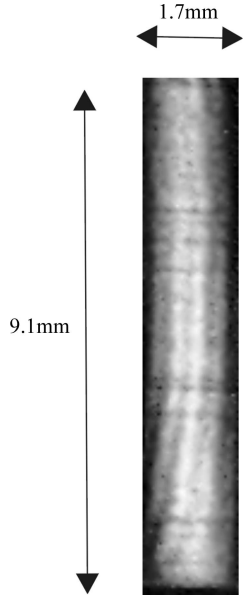

Figure 7
Constant-thickness fringes x = constant obtained in the hard X-ray interferometer with a wedge placed in one of the arms of the interferometer.

In addition, a controllable moiré is obtained with the hard interferometer when a Plexiglass wedge is placed in one of the arms of the interferometer (Fig. 7). The apex of the wedge is vertically aligned and the wedge slope is horizontally oriented. The moiré fringes (constant-thickness lines x = constant) are perpendicular to the diffraction plane. The hard interferometer is freely placed on the goniometer head. As we see in Fig. 7, the fringes are slightly curved. Perhaps this is because the edges of the used wedge are not perfectly flat. The period of the fringes is approximately $2\pi/[k(1 - n)\tan\varepsilon]$, where $k = 2\pi/\lambda$, λ is the wavelength, n is the refractive index of the wedge and ε is the wedge angle at the apex. We used a wedge with $\varepsilon \simeq 2^\circ$. The estimated period is approximately 1 mm, which coincides with the obtained fringe period.

3. Conclusions

In this work, a new 'hard' X-ray interferometer is tested for experimental investigations. In comparison with the usual X-ray interferometer, this type of interferometer not only has a base but also a ceiling. Due to this construction, the hard X-ray interferometer does not produce an uncontrollable moiré caused by uncontrollable deformations in the interferometer plates. We obtained a uniform intensity distribution in the interfering beams.

Experimentally, it is shown that the hard interferometer must be freely placed on the goniometer head because the interferometer is very sensitive to minor mechanical stresses. Therefore, the alignment conditions for the hard interferometer are much more stringent than for a conventional interferometer.

Also, constant-thickness fringes are obtained, using a wedge placed in one of the arms of the hard interferometer. The apex of the wedge is vertically placed.

It should be noted that the volumes where a test sample can be inserted are limited. This is due to the fact that the hard interferometer has not only a base but also a ceiling. When manufacturing such interferometers in the future, it is necessary to increase these volumes, taking the mentioned inconvenience into consideration if possible.

The main conclusion is that such a type of hard X-ray LLL interferometer can be successfully used for experimental investigations of objects and deformations. This will be an alternative method to the fringe scanning method. The results obtained by means of these two methods can be compared. One of the specific applications of the hard X-ray interferometer will be coherent interferometric Fresnel and Fourier holographies. The excellence of the hard interferometer rests in the controllability of the moiré fringes (there is no uncontrollable preliminary moiré). The above-

mentioned difficulties are not fundamental and they can be overcome.

References

Authier, A. (2001). *Dynamical Theory of X-ray Diffraction*. Oxford University Press.
Balyan, M. K. (2016*a*). *J. Contemp. Phys.* **51**, 79–88.
Balyan, M. K. (2016*b*). *J. Contemp. Phys.* **51**, 289–298.
Bonse, U. & Hart, M. (1965*a*). *Appl. Phys. Lett.* **6**, 155–156.
Bonse, U. & Hart, M. (1965*b*). *Appl. Phys. Lett.* **7**, 99–100.
Eyramjyan, T. H., Mnatsakanyan, T. S. & Balyan, M. K. (2018). *Acta Cryst.* A**74**, 595–599.
Ingal, V. L. & Beliaevskaya, E. A. (1995). *J. Phys. D Appl. Phys.* **28**, 2314–2317.
Momose, A. (1995). *Nucl. Instrum. Methods Phys. Res. A*, **352**, 622–628.
Momose, A. & Hirano, K. (1999). *Jpn. J. Appl. Phys.* **38**, 625–629.
Pinsker, Z. G. (1982). *X-ray Crystallooptics*. Moscow: Nauka.
Rostomyan, A., Mesropyan, M., Narimanyan, S. & Grigoryan, A. (1989). USSR Patent SU 1458781 A1.